

**Sequential cytoprotective responses to Sigma1 ligand induced endoplasmic reticulum
stress**

Joel M. Schrock, Christina M. Spino, Charles G. Longen, Stacy M. Stabler, Jacqueline C.

Marino, Gavril W. Pasternak, Felix J. Kim

Department of Pharmacology & Physiology, Drexel University College of Medicine,

Philadelphia, PA 19102: CMS, CGL, FJK

Molecular Pharmacology and Chemistry Program, Memorial Sloan-Kettering Cancer Center,

New York, NY 10065: JMS, SMS, JCM, GWP

Running title: Sigma1 ligand induced UPR and autophagy

Address correspondence to:

Felix J. Kim, PhD
Department of Pharmacology & Physiology
Drexel University College of Medicine
245 North 15th Street
Philadelphia, PA 19102-1192
fkim@drexelmed.edu
tel: 215-762-2508
fax: 215-762-2299

Document Statistics:

Text pages: 39
Tables: 0
Figures: 8
Supplemental Figures: 4
References: 54
Abstract word count: 240
Introduction word count: 750
Discussion word count: 1,479

List of nonstandard abbreviations:

UPR, unfolded protein response; IRE1alpha, inositol-requiring enzyme 1 alpha; eIF2alpha, eukaryotic initiation factor 2 alpha; GRP78/BiP, 78 kilodalton glucose-regulated protein, also known as binding immunoglobulin protein; ATF4, activating transcription factor 4; PARP, Poly (ADP-ribose) polymerase, GFP: green fluorescent protein; LC3, microtubule-associated protein 1 light chain 3; ATG5, autophagy protein 5; PGRMC1, progesterone receptor membrane component 1

ABSTRACT

The Sigma1 receptor (Sigma1) is an endoplasmic reticulum (ER) integral membrane protein that is highly expressed in a number of cancer cell lines. Small molecule compounds targeting Sigma1 (Sigma1 ligands) inhibit cancer cell proliferation and induce apoptotic cell death in vitro and inhibit tumor growth in xenograft experiments. However, the cellular pathways activated by Sigma1 protein-ligand interaction are not well defined. Here, we find that treatment with some Sigma1 ligands induces ER stress and activates the unfolded protein response (UPR) in a dose and time responsive manner in a range of adenocarcinoma cell lines. Autophagy is engaged following extended treatment with Sigma1 ligands, suggesting that protracted UPR results in autophagy as a secondary response. Inhibition of UPR by RNAi mediated knockdown of IRE1 α and ATF4 abrogates autophagosome formation, as does knockdown of essential autophagy gene products Beclin1 and ATG5. Knockdown of Sigma1 also suppresses IPAG induced UPR marker and autophagosome levels, indicating that this response is indeed Sigma1 mediated. We find that UPR activation precedes autophagosome formation and autophagy precedes apoptosis in Sigma1 ligand treated cells. These processes are reversible, and wash-out of IPAG prior to cell death results in a return of autophagosomes and UPR markers toward basal levels. However, inhibition of Sigma1 ligand induced UPR or autophagy accelerates apoptotic cell death. Together, these data suggest that UPR and autophagy are engaged as primary and secondary cytoprotective responses, respectively, to Sigma1 ligand induced disruption of cancer cell protein homeostasis.

INTRODUCTION

In eukaryotic cells the endoplasmic reticulum (ER) is the primary site of synthesis, folding, and assembly of secreted and integral membrane proteins and their macromolecular complexes (Ron and Walter, 2007). Maintenance of ER protein homeostasis relies on the timely convergence of multiple pathways that detect homeostatic protein concentration thresholds and control the ebb-and-flow of ER proteins (Jonikas et al., 2009; Mu et al., 2008; Ron and Walter, 2007). Disruption of ER homeostasis activates stress response pathways including the unfolded protein response (UPR) (Kim et al., 2008; Ron and Walter, 2007; Xu et al., 2005). The mammalian UPR comprises at least two phases: an initial alarm phase followed by a cytoprotective, adaptive phase in which UPR factors are up-regulated to enhance the cellular capacity to process increased concentrations of unfolded protein (Kim et al., 2008; Marciniak and Ron, 2006; Ron and Walter, 2007).

It has been proposed that severe or prolonged ER stress can overwhelm the UPR and the cell may engage autophagy as a secondary survival response (Bernales et al., 2006; Bernales et al., 2007; Ogata et al., 2006; Ron and Walter, 2007; Yorimitsu et al., 2006). Growing evidence suggests that ER stress, the unfolded protein response, and autophagy are likely integrated signaling pathways that modulate cell survival and growth (He and Klionsky, 2009; Hoyer-Hansen and Jaattela, 2007; Levine and Klionsky, 2004; Ron and Walter, 2007).

Autophagy describes a set of bulk cellular degradation pathways by which cells can maintain energy levels under conditions of metabolic stress as well as a mechanism by which large aggregates of mis-folded proteins and damaged cellular components, including damaged organelles, are sequestered into membrane bound vesicles called autophagosomes and subsequently targeted for lysosomal degradation (Levine and Klionsky, 2004; Levine and

Kroemer, 2008; Mizushima et al., 2008). Thus, autophagy plays important roles in the maintenance of cellular homeostasis and disease prevention, and defective autophagy pathways have been implicated in pathologies including neurodegenerative disease and cancer (Levine and Kroemer, 2008; Mathew et al., 2009; Mizushima et al., 2008). Autophagy may serve a cytoprotective role in cancer cells that allows survival under the challenging metabolic conditions of the tumor cell environment (Degenhardt et al., 2006; Levine and Kroemer, 2008; Mathew et al., 2009; Mizushima et al., 2008). Furthermore, protein degradation mechanisms such as autophagy may serve to mitigate the higher intrinsic levels of proteotoxic stress in tumor cells (Solimini et al., 2007). Several chemotherapeutic agents have been shown to induce autophagy (Rubinsztein et al., 2007). However, in many cases it remains unclear whether cell death occurs by autophagy, whether cell death is associated with autophagy, or whether autophagy is a survival response to cytotoxic chemotherapy (Hippert et al., 2006; Levine and Klionsky, 2004; Levine and Kroemer, 2008; Mathew et al., 2009). Emerging data suggest that autophagy participates in integrated responses to cellular stress that determine cell death versus survival. The proteins and pathways that regulate these integrated stress responses are just beginning to be clearly defined (He and Klionsky, 2009; Hoyer-Hansen and Jaattela, 2007; Levine and Klionsky, 2004; Ron and Walter, 2007).

Although first proposed as members of the opioid receptor family based upon their affinity for an opioid-related ligand (Martin et al., 1976), sigma receptors are now considered distinct binding sites unrelated to any classical receptors. The cloned sigma1 receptor (Sigma1) predicts a 26-kilodalton integral membrane protein that is enriched in the ER (Aydar et al., 2002; Hanner et al., 1996; Hayashi and Su, 2007). Sigma1 has been proposed to function as a molecular

chaperone at the ER-mitochondrion interface in certain cell types (Hayashi and Su, 2007). However, the physiological role of Sigma1 in tumor cells remains unclear.

Sigma1 is highly expressed in various tumor cell lines, including breast and prostate adenocarcinoma (Aydar et al., 2006; Spruce et al., 2004; Vilner et al., 1995b). Some Sigma1 ligands may be effective anti-tumor agents (Berthois et al., 2003; Piergentili et al.; Spruce et al., 2004; Vilner et al., 1995a). Some Sigma1 ligands inhibit cell proliferation, induce apoptotic cell death in vitro, and inhibit tumor growth in mouse tumor xenograft experiments (Berthois et al., 2003; Spruce et al., 2004). However, the mechanisms of Sigma1 mediated actions remain largely unknown. In vitro, ligand treatment results in apoptotic cell death following extended treatment, with time and dose depending on the compound and cell line (Berthois et al., 2003; Piergentili et al.; Spruce et al., 2004; Vilner et al., 1995a). Here we asked whether Sigma1 ligand treatment induces cascades of cytoprotective signaling in response to ligand induced disruption of ER protein homeostasis.

MATERIALS AND METHODS

Chemicals. Sigma1 ligands, IPAG (1-(4-Iodophenyl)-3-(2-adamantyl) guanidine), haloperidol hydrochloride (4-[4-(4-Chlorophenyl)-4-hydroxy-1-piperidinyl]-1-(4-fluorophenyl)-1-butanone hydrochloride), PRE-084 hydrochloride (2-(4-Morpholinethyl) 1-phenylcyclohexanecarboxylate hydrochloride), (+)SKF10047 hydrochloride ([2S-(2a,6a,11R*)-1,2,3,4,5,6-hexahydro-6,11-dimethyl-3-(2-propenyl)-2,6-methano-3-benzazocin-8-ol hydrochloride), and (+)pentazocine were obtained from Tocris or the National Institute on Drug Abuse. Bafilomycin A1, inhibitor of the vacuolar type H⁺-ATPase (V-ATPase), and thapsigargin were purchased from Sigma Aldrich.

Cell lines and transfections. The MDA-MB-468, T47D, MCF7 breast adenocarcinoma, PC3, prostate adenocarcinoma, Panc1 pancreatic adenocarcinoma, and HepG2 hepatocellular carcinoma cell lines were all acquired from ATCC. Cells were maintained in a 1:1 mixture of DMEM:F-12 with 4.5 g/liter glucose, 5% fetal bovine serum, non-essential amino acids and penicillin/streptomycin. Cells were seeded approximately 24 hours prior to start of drug treatment in most assays. Human Beclin1, human Sigma1, human PGRMC1, human IRE1 α , human ATF4, and Control-A siRNA were purchased from Santa Cruz Biotechnology and human ATG5 siRNA was purchased from Cell Signaling Technologies. siRNA transfections (100 nanomoles per 35mm well) were performed with Oligofectamine (Invitrogen) or INTERFERin (PolyPlus) transfection reagent according to manufacturer's procedures. Cells were treated with indicated drugs 72 hours post-transfection for all RNA interference experiments, except Sigma1, PGRMC1, and ATG5. For Sigma1, PGRMC1, and ATG5 siRNA knockdown, 100 nanomoles of siRNA per approximately 100,000 cells was transfected with INTERFERin transfection reagent

(PolyPlus), and 48 hours later, cells were reseeded, allowed to attach and recover for at 16 -to- 24 hours and transfected again. Twenty-four hours following the second transfection of these siRNA, cells were treated with IPAG for 12 -to- 24 hours, as indicated. Transfection of Control-A siRNA (Santa Cruz Biotechnology) was performed in parallel, using the conditions described above.

Cell death assays. We evaluated cell death by trypan blue exclusion assay, propidium iodide staining, as well as cleaved caspase 3 (Asp 175) and cleaved PARP (Asp 214) immunoblot. Trypan blue exclusion and propidium iodide staining were used to quantify general cell death and the presence of apoptotic cell death was confirmed by immunoblot. Values were generated from at least 6 independent determinations, and statistical significance was determined as described below.

Immunoblots and antibodies. Cells were lysed and proteins extracted in a modified RIPA buffer (25 mM Tris-HCl pH 7.6, 150 mM NaCl, 1% NP-40, 1% sodium deoxycholate and 0.1 % SDS) supplemented with 10% glycerol (volume/volume), Complete protease inhibitor cocktail (Roche), and Halt phosphatase inhibitor cocktail (Pierce). Approximately 10-20 μ g of detergent soluble protein were resolved on precast NOVEX polyacrylamide Tris-glycine gels (InVitrogen). Immunoblots were performed in a 20 mM Tris-buffered 137 mM saline solution (pH 7.6) containing 0.1% Tween-20 (polyoxyethylene (20) sorbitan monolaurate) and 5% (weight/volume) blotting grade non-fat dry milk (BioRad). All washes were performed in the same buffer without the blotting grade non-fat dry milk. The Lumigen PS-3 enhanced chemiluminescence kit (GE Healthcare) was used to reveal immunoblotted proteins. The rabbit

anti-Sigma1 antibody was generated in our laboratory as described elsewhere (Kim et al., 2012). The anti-GFP, anti- β -actin, anti-Beclin1, anti-ATF4, anti-PGRMC1, and all horseradish peroxidase conjugated secondary antibodies were purchased from Santa Cruz Biotechnologies. The anti-LC3B, anti-ATG5, anti-phospho-p38MAPK (Thr180/Tyr182), anti-phospho-SAPK/JNK (Thr183/Tyr185), anti-IRE1 α , anti-PERK, anti-phospho-eIF2 α (Ser51), anti-GRP78/BiP, anti-cleaved caspase 3 (Asp 175), and anti-cleaved PARP (Asp 214) were all purchased from Cell Signaling Technologies.

Microscopy and quantification of autophagosome formation. The human GFP-LC3 expression plasmid, pEGFP-LC3 (a gift from Drs. Grazia Ambrosini and Gary K. Schwartz, MSKCC), was stably transfected into MDA-MB-468 and selected with 0.5 mg/ml G418 sulfate. Stable populations were generated and compared to parental MDA-MB-468 for Sigma1 expression and autophagic and growth inhibitory response to Sigma1 ligands. GFP-LC3 translocation (puncta formation) was assessed by microscopy and autophagic degradation (flux) was assessed by an immunoblot based GFP-LC3 cleavage assay in MDA-MB-468(GFP-LC3) stable cell populations. For microscopy-based experiments, cells were seeded onto Lab-Tek II glass chamber slides (Nalge Nunc International). Following the indicated number of hours of drug treatment, cells were washed with room temperature Dulbecco's modified phosphate buffered saline solution, containing calcium and magnesium, and fixed and permeabilized with room temperature BD Cytotfix-Cytoperm solution (BD Biosciences). Images of GFP-LC3 puncta were acquired with a Zeiss Axioplan 2 Imaging widefield microscope using Axiovision LE software. Puncta were counted using the spot quantification program in the Fluoro-Chem software package (Alpha Innotech) and confirmed in parallel by manual counting.

Autophagic flux assays. We evaluated autophagic flux (turnover of autolysosome cargo) using two previously described methods (Bernales et al., 2006; Hosokawa et al., 2006; Klionsky et al., 2008; Mizushima and Yoshimori, 2007). Lipid-conjugated GFP-LC3 translocates to autophagosomes that conditionally fuse with lysosomes, leading to autolysosomal degradation of LC3 and release of GFP in the case of active autophagic flux (Bernales et al., 2006; Hosokawa et al., 2006). In this GFP-LC3 degradation assay, cleaved GFP was detected by immunoblot (Bernales et al., 2006; Hosokawa et al., 2006). Autophagic flux was also verified by inhibiting autolysosomal degradation with the specific inhibitor of the vacuolar type H⁺-ATPase, Bafilomycin A1. In this assay, absence of cleaved and released GFP is an indicator that ligand induced autophagic flux has been inhibited by Bafilomycin A1 (Klionsky et al., 2008; Mizushima and Yoshimori, 2007).

Sigma1 ligand binding assay. Radioactive [¹²⁵I]IPAG was synthesized essentially as described previously (Kimes et al., 1992) and subsequently purified and confirmed against cold standard by high-performance liquid chromatography. Protein concentrations for the Sigma1 binding assay were determined by modified Lowry assay, as described previously (Ryan-Moro et al., 1996; Wolozin et al., 1982). The [¹²⁵I]IPAG saturation binding assays were performed by incubating the membranes for 90 min for 25°C in potassium phosphate buffer (50 mM, pH 7.4) containing magnesium sulfate (5 mM). Whatman GF/B filters were presoaked for 30 minutes in 0.5% polyethylenimine. After incubation, the reaction mix was filtered onto presoaked Whatman GF/B filters using a Brandel cell harvester (Brandel, Gaithersburg, MD). Nonspecific binding was determined in presence of unlabeled haloperidol (1 mM). Specific binding was defined as the

difference between total and nonspecific binding. Filter bound radioactivity was detected using a gamma counter (PerkinElmer Life and Analytical Sciences, Waltham, MA). Binding saturation curves were generated using nonlinear regression analysis (Prism, GraphPad Software Inc., San Diego, CA).

Statistical analysis. Statistical significance was determined by one-way ANOVA followed by Bonferroni's post-test using Prism software (GraphPad).

RESULTS

Some Sigma1 ligands induce autophagosome formation and autophagic flux. MDA-MB-468 and T47D breast adenocarcinoma cells, which natively express Sigma1 (Spruce et al., 2004), were treated with 10 μ M of the following small molecule compounds with binding affinity for Sigma1 (herein referred to as Sigma1 ligands): IPAG, haloperidol, PRE-084 (PRE), and (+)SKF10047. In all of our experiments we noticed that some Sigma1 ligands, the putative antagonists, decreased cell size by approximately 16 to 24 hours after treatment ((Kim et al., 2012) and shown for 24 hour treatment of MDA-MB-468 in Supplemental Figure 1). In view of evidence that autophagy plays a role in cell growth (Hosokawa et al., 2006; Scott et al., 2007), we evaluated the potential involvement of this bulk sequestration and degradation process in Sigma1 ligand-mediated decrease in cell size. Initially, we tested for the activation of autophagy using an established immunoblot-based assay to detect microtubule associated protein light chain 3 (LC3) lipidation (Klionsky et al., 2008; Mizushima and Yoshimori, 2007). In these experiments treatment with Sigma1 putative antagonists (IPAG, haloperidol), but not agonists (PRE-084, (+)SKF10047), converted LC3 to LC3II, an indication of LC3 lipid conjugation and autophagosome formation (Fig. 1G). We confirmed these results with a widely used microscopy-based assay to visualize and quantify the translocation of an amino-terminal green fluorescent protein tagged LC3 (GFP-LC3) into vesicular structures which appear as GFP-concentrated puncta characteristic of autophagosome formation (Klionsky et al., 2008). Since transient transfections can produce spurious GFP-LC3 aggregates (Klionsky et al., 2008; Kuma et al., 2007), we generated stable GFP-LC3 transfected populations of MDA-MB-468(GFP-LC3). These cells were treated for 24 hours with 10 μ M Sigma1 putative antagonists (IPAG, haloperidol) and 10 μ M or 50 μ M putative agonists (PRE-084, (+)SKF10047 – data shown for

50 μ M of each), and were compared to basal (non-treated) and DMSO treated controls (Fig. 1A, B). Autophagosome formation in MDA-MB-468(GFP-LC3) cells was quantified as the mean number of GFP-LC3 puncta per GFP-positive cell. In the microscopy-based assay, we found that among the four ligands tested, only IPAG and haloperidol significantly induced the formation of autophagosomes (Fig. 1). Treatment with 10 μ M IPAG or haloperidol for 24 hours resulted in 23 ± 2 and 29 ± 4 puncta per cell, respectively (Fig. 1B). Basal and DMSO treated cells produced less than 8 puncta per cell (Fig. 1). The putative agonists PRE-084, (+)SKF10047, and (+)pentazocine produced less than 8 puncta per cell, at drug concentrations up to 50 μ M (data shown for PRE-084 and (+)SKF10047 in Fig.1), and thus did not significantly differ from basal or DMSO control in this assay.

To determine whether Sigma1 antagonists induce autolysosomal degradation of cargo proteins (autophagic flux (Klionsky et al., 2008)), we used an immunoblot-based assay to detect and quantify LC3 degradation (Bernales et al., 2006; Hosokawa et al., 2006; Klionsky et al., 2008; Mizushima and Yoshimori, 2007). We evaluated autophagic flux in Sigma1 ligand treated cells by detecting the conversion of GFP-LC3 to a lipid-conjugated form, GFP-LC3II, and subsequent cleavage of GFP-LC3II. In the presence of active autophagic degradation (flux), LC3 is degraded in the autolysosome, whereas cytoplasmic GFP, which is relatively resistant to degradation, is cleaved and released from LC3 and can be detected as free GFP by immunoblot (Bernales et al., 2006; Hosokawa et al., 2006). IPAG and haloperidol increased GFP-LC3II levels and cleaved GFP (Fig. 1C). The lower band, immediately below the prominent GFP-LC3 band, is the lipid-conjugated form of GFP-LC3, GFP-LC3II (Bernales et al., 2006; Hosokawa et al., 2006). In contrast to Sigma1 putative antagonist-induced GFP-LC3II conversion and cleavage, neither the putative agonist PRE-084 nor (+)SKF10047 increased levels of GFP-LC3II

or cleaved GFP at concentrations up to 50 μ M (Fig. 1C). However, in the presence of a small molecule inhibitor of autophagic degradation, vacuolar type H⁺-ATPase inhibitor Bafilomycin A1 (Baf A1), the combination of Baf A1 with IPAG decreased GFP-LC3 cleavage and release of cleaved GFP, suggesting suppression of autophagic flux (Fig. 1D-F). Moreover, a supplemental increase in GFP-LC3 positive puncta in the presence of Baf A1 further indicated enhanced autolysosomal degradation in IPAG treated cells (Fig. 1D-F).

Finally, using the immunoblot based LC3II conversion assay, we found that IPAG induces autophagy in at least 5 other cancer cell lines, including two breast adenocarcinoma, one prostate adenocarcinoma, one pancreatic adenocarcinoma, and one hepatocellular carcinoma cell line (Fig. 1H).

Sigma1 ligand induced autophagy requires essential autophagy genes. Autophagy is a specific, highly regulated process that requires a series of essential autophagy gene products (He and Klionsky, 2009; Levine and Klionsky, 2004). To confirm that GFP-positive puncta formation and degradation were indeed products of autophagy, we evaluated the effects of RNAi mediated knockdown of Beclin1 and ATG5, both essential autophagy proteins (Levine and Klionsky, 2004). Knockdown of Beclin1 significantly inhibited puncta formation, decreasing the mean number of puncta per cell from 28 ± 3 to 6 ± 1 in IPAG treated cells, an 80% inhibition of IPAG-induced GFP-LC3 puncta formation ($p < 0.001$) Fig. 2A-C). Knockdown of ATG5 inhibited IPAG induced puncta formation by approximately 60%, decreasing the mean number of IPAG induced puncta per cell from 33 ± 2 in control siRNA transfected cells to 14 ± 1 in cells in which ATG5 was knocked-down ($p < 0.001$) (Fig. 2D-F).

Sigma1 ligand disrupts endoplasmic reticulum protein homeostasis and activates stress associated unfolded protein response. We subsequently asked whether treatment with the Sigma1 putative antagonist, IPAG, immediately induces autophagy or whether it is activated downstream of other cellular events. Sigma1 is highly enriched in the endoplasmic reticulum and has been recently described to function as a molecular chaperone at the ER-mitochondrion interface (Hayashi and Su, 2007). Therefore, we asked whether Sigma1 ligand treatment could disrupt ER protein homeostasis and induce ER stress. ER stress is commonly associated with an accumulation of unfolded and/or mis-folded proteins, and thus activates stress response pathways including the unfolded protein response (UPR) (Ron and Walter, 2007; Schroder and Kaufman, 2005; Xu et al., 2005). The UPR comprises several signaling pathways that increase the protein folding and processing capacity of the ER. The three most extensively investigated sensors that initiate the UPR, IRE1 α , PERK, and ATF6 transduce signals to a cascade of effectors (Ron and Walter, 2007; Schroder and Kaufman, 2005; Xu et al., 2005). Many of these UPR effectors function as transcription factors that induce the synthesis of ER chaperones involved in maintaining protein homeostasis (Ni and Lee, 2007; Ron and Walter, 2007; Schroder and Kaufman, 2005; Xu et al., 2005). We assayed for the IRE1 α -JNK1/2 and PERK-eIF2 α -ATF4 components of the UPR as well as UPR-associated ER chaperone, GRP78/BiP (BiP), as indicators of activated UPR (Ni and Lee, 2007; Ogata et al., 2006; Ron and Walter, 2007; Schroder and Kaufman, 2005; Xu et al., 2005).

The stress induced mitogen activated protein kinase p38 (p38MAPK) is a downstream target of the IRE1-TRAF2 (TNF receptor-associated receptor 2)-ASK1 (apoptosis signaling regulated kinase 1) signaling complex that is activated in response to ER stress and subsequently phosphorylates and enhances apoptosis (Kim et al., 2008; Ron and Walter, 2007; Szegezdi et al.,

2006; Xu et al., 2005). In addition, a recent report also demonstrates a role for p38MAPK in the control of macroautophagy (Webber and Tooze, 2010)

We evaluated all of the above-mentioned markers of ER stress following treatment with increasing doses of Sigma1 ligands in order to compare UPR with the dose-responsive activation of autophagy, described above. We found that Sigma1 putative antagonists activate the UPR in a dose-responsive manner (data shown for IPAG in Fig. 3). In contrast, Sigma1 putative agonists did not activate any of these markers (data not shown). Interestingly, the unfolded protein response to IPAG induced endoplasmic reticulum stress (Fig. 3) occurs at lower doses than the autophagic response (Fig. 2). Indeed treatment with 1 μ M IPAG, a dose that does not produce autophagosomes, resulted in a salient and significant activation of at least seven markers of UPR (Fig. 3). Whereas the mean EC_{50} of LC3 lipid conjugation (i.e., LC3II induction) is 7 μ M, the EC_{50} values for induction of ATF4, IRE1 α , BiP, and phosphorylation of eIF2 α (Ser51), JNK (Thr183/Tyr185), and p38MAPK (Thr180/Tyr182) are 0.5, 0.9, 1.4, 2.3, 1.6, 1.7, and 0.5 μ M, respectively. These mean values were generated from two independent determinations. Phosphorylated PERK, indicated by decreased electrophoretic mobility compared to non-phosphorylated PERK, could be detected following treatment with 1 μ M IPAG (Fig. 3). Together, these data demonstrate that Sigma1 antagonist induction of UPR occurs at 3 to 14 fold lower concentrations than required for autophagosome formation (Fig. 3).

Next, we asked whether autophagy occurs prior or subsequent to UPR. Cells were treated with 10 μ M IPAG for 1, 6, 12, and 24 hours (Fig. 4). Of the seven ER stress and UPR markers evaluated in this experiment, salient induction of 5 was detected by 1 hour of treatment, and 3 were clearly induced between 1 to 6 hours (Fig. 4A-D). In contrast, significant formation of autophagosomes, measured by GFP-LC3 puncta and LC3II immunoblot, was detected between 6

to 12 hours (Fig. 4E). Clearly, UPR is induced prior to the detectable formation of autophagosomes.

Despite the activation of stress markers and increase in JNK phosphorylation, we observed no change in steady-state BCL2 protein levels up to 24 hours of treatment with 10 μ M IPAG (Fig. 4F). However, when treatment was extended to 48 hours, we observed a marked decrease BCL2 (data not shown), consistent with the appearance of apoptotic cell death at this treatment time point (Fig. 7).

Finally, we found that IPAG induces UPR in a range of cancer cell lines, including at least two other breast adenocarcinoma (T47D and MCF-7), one prostate adenocarcinoma (PC3), one pancreatic adenocarcinoma (Panc1), and one hepatocellular carcinoma cell line (HepG2) (Fig. 4G).

Sigma1 ligand induced UPR and autophagy are suppressed by Sigma1 RNAi. To confirm that the Sigma1 ligand induced UPR and autophagy are indeed Sigma1 mediated, we used siRNA to knockdown Sigma1 in MDA-MB-468(GFP-LC3) cells, and evaluated IPAG-induced autophagy (Fig. 5). Significant Sigma1 knockdown was detectable >90 hours after transfection of Sigma1 selective siRNA, suggesting a stable, long protein half-life, consistent with previous reports (Hayashi and Su, 2007). We found that approximately 60% knockdown of Sigma1 resulted in a corresponding decrease of [¹²⁵I]IPAG binding in a radioligand binding saturation assay, decreasing maximal IPAG binding (B_{max}) from 1837 fmol/mg to 748 fmol/mg, demonstrating the selectivity of the siRNA knockdown and of IPAG (Fig. 5A). In our functional assays we were able to knockdown Sigma1 to approximately 20% of basal levels (Fig. 5B-D). Consistent with Sigma1-mediated effects of IPAG, we found that approximately 80% knockdown of Sigma1

resulted in suppression of IPAG induce UPR, evaluated by induction BiP, IRE1 α , and ATF4 protein levels (Fig. 5B). We subsequently evaluated autophagosome formation (GFP-LC3 puncta). Knockdown of Sigma1 alone did not induce the formation of autophagosomes in the absence of Sigma1 ligand, 6 ± 2 puncta per cell compared to 7 ± 3 puncta per cell in control siRNA transfected cells (Fig. 5C-D). Treatment with 10 μ M IPAG resulted in 28 ± 4 puncta per cell in control siRNA transfected cells and a significant inhibition to 10 ± 2 puncta per cell in Sigma1-knockdown cells (Fig. 5C-D). Together, these data demonstrate that Sigma1 is required for both IPAG induced UPR and autophagy.

Inhibition of UPR suppresses Sigma1 ligand induced autophagy. The results of our dose-response and time-action experiments suggest that ER stress-induced UPR is engaged upstream of autophagy; however, they do not demonstrate that ER stress is required to activate autophagy. Therefore, we subsequently tested the effects of inhibiting the ER stress response to Sigma1 antagonist treatment. To confirm that UPR precedes and is required for Sigma1 antagonist-induced autophagy, we inhibited UPR by siRNA-mediated knockdown of IRE1 α or ATF4. In these experiments, after transfection of siRNA, MDA-MB-468 cells were treated for 24 hours with 10 μ M IPAG (Fig. 6). Knockdown of IRE1 α resulted in decreased autophagosome formation (Fig. 6A,C,D). The number of GFP-positive puncta per cell decreased from 24 ± 2 and 33 ± 2 , respectively, when treated with IPAG or haloperidol alone to 9 ± 2 and 13 ± 2 , respectively, when IRE1 α was knocked down (Fig. 6C,D). When siRNA was used to knockdown ATF4, IPAG or haloperidol treatment produced 5 ± 1 and 15 ± 2 GFP-positive puncta per cell, respectively (data shown for IPAG in Fig. 6B,C,D). Together, these data suggest that Sigma1 ligand induced autophagy occurs via UPR activation.

Inhibition of Sigma1 ligand induced UPR and autophagy accelerate apoptotic cell death. The results described above suggest that UPR and autophagy may function as primary and secondary survival responses, respectively, to Sigma1 ligand induced ER stress. Previous studies with tunicamycin and thapsigargin have demonstrated that ER stress can lead to autophagy as a survival response (Ogata et al., 2006; Yorimitsu et al., 2006). Following 24 hours of treatment with IPAG and haloperidol, ligand induced MDA-MB-468 cell death was not significantly different than untreated (basal) or DMSO treated controls, with $10 \pm 2\%$ and $10 \pm 3\%$ dead cells per well, respectively, compared to $9 \pm 1\%$ dead cells in DMSO treated control samples (data for IPAG shown in Fig. 7). DMSO treated control cell death was not significantly different than untreated or basal cell death rates. However, following 48 hours of continuous treatment, a significant percentage of IPAG treated cells begin to undergo apoptotic cell death, with an average of $30 \pm 2\%$ of the cells dying under these conditions (Fig. 7A,B). By 72 hours of treatment with IPAG $> 75\%$ of cells died. Consistent with this pattern, whereas control siRNA transfected cells survived 24 hours of IPAG and haloperidol treatment, with $9 \pm 4\%$ and $7 \pm 2\%$ dead cells per well, respectively, inhibition of UPR by IRE1 α knockdown potentiated IPAG and haloperidol induced cell death with $47 \pm 8\%$ and $61 \pm 8\%$ dead cells, respectively, following 24 hours of Sigma antagonist treatment (Fig. 7C,D). Knockdown of ATF4 also potentiated IPAG and haloperidol induced apoptosis with $30 \pm 9\%$ and $53 \pm 11\%$ dead cells per well, respectively, whereas ATF4 knockdown alone did not significantly alter cell death rates, with $7 \pm 2\%$ dead cells per well (data not shown). Thus, inhibition of UPR by siRNA knockdown of IRE1 α or ATF4 abrogates autophagosome formation (Fig. 6) and potentiates Sigma1 antagonist-mediated apoptotic cell death (Fig. 7, data shown for IRE1 α).

To determine whether Sigma1 ligand induced autophagy functions as a cell death or survival pathway, or whether autophagy is simply associated with Sigma1 ligand induced cell death, we evaluated the effects of inhibiting autophagy by siRNA mediated Beclin1 or ATG5 knockdown. Whereas treatment with 10 μ M IPAG for 24 hours does not induce significant cell death ($5 \pm 3\%$), with no evidence of apoptosis, inhibiting autophagosome formation by siRNA knockdown of Beclin1 or ATG5 results in cell death at 24 hours of IPAG treatment (Fig. 7 and Supplemental Figure 2, respectively).

Sigma1 ligand induced UPR and autophagy are reversible. Interestingly, removal of Sigma1 ligand prior to activation of cell death pathways results in a rapid disappearance of autophagosomes (Fig. 8A-C). Thus, Sigma1 ligand induced autophagy is rapidly reversible if it is removed prior to progression beyond an irreversible cytoprotective threshold. Whether our observations reflect a sequestration and subsequent recycling after removal of drug or degradation of autophagosome cargo remains unclear. The absence of cell death during this treatment period was confirmed by trypan blue exclusion assay (Fig. 8E). These data suggest that constant treatment, and presumably constant ligand-receptor binding, is required for antagonist-induced stress response and autophagy. Upon removal (“wash-out”) of IPAG from the cell culture medium, UPR markers returned to basal levels at various time frames: within 1 -to- 6 hours for PERK, phospho-eIF2 α , and phospho-p38MAPK; 6 -to- 24 hours for ATF4; 24 -to- 48 hours for IRE1 α and BiP (Fig. 8D). Thus, UPR is engaged prior to autophagy and remains active for several hours after autophagy subsides, suggesting that UPR may act to maintain ER homeostasis at lower intensity of stress. The activation of these signaling pathways, and likely others, suggests an integrated response to Sigma1 ligand induced ER stress. Furthermore, the

reversibility of autophagy and UPR, subsequent to wash-out of IPAG, supports the notion that these are cytoprotective responses.

DISCUSSION

A growing number of reports suggest that autophagy may be part of an integrated response to cellular stress (He and Klionsky, 2009; Hoyer-Hansen and Jaattela, 2007; Kim et al., 2008; Levine and Klionsky, 2004; Ron and Walter, 2007). Our findings suggest a role for Sigma1 in this process. Here we demonstrate that high affinity Sigma1 ligands induce ER stress and subsequent UPR (Fig. 3-4). Severe or prolonged ligand induced ER stress appears to overwhelm the cytoprotective, adaptive capacity of the UPR and the cell subsequently engages autophagy. RNAi knockdown of Sigma1 suppresses IPAG induced UPR and autophagy (Fig. 5), suggesting that Sigma1 is the principal mediator of these ligand induced ER stress responses.

Treatment with two Sigma1 putative antagonists (IPAG, haloperidol) resulted in the activation of UPR and autophagosome formation whereas putative agonists (PRE-084, (+)SKF10047) did not induce either. Our results are consistent with published data demonstrating that putative antagonists mediate cell death whereas putative agonists do not elicit a detectable cytotoxic response (Spruce et al., 2004). One possible explanation for the absence of putative agonist effect may be the predominance of Sigma1 in a constitutive agonist conformation in cancer cells. Alternatively, because IPAG and haloperidol associated autophagosome formation is not blocked by PRE-084 and (+)SKF10047 (Kim et al, unpublished observations), it is possible that putative antagonists and agonists bind to distinct Sigma1 populations within the cell, or it is possible that they bind to distinct regions of Sigma1 and thereby elicit different effects even when bound to the same protein. Interestingly, it appears that binding affinity does not necessarily predict drug actions as ligands with similar affinities elicit distinct responses (Fig. 1). Among the ligands used here, we find that IPAG binds Sigma1 with high affinity, K_d 3 nM (Fig. 5), and we have previously determined the Sigma1 binding affinity

of haloperidol as K_d 4 nM (Ryan-Moro et al., 1996). PRE-084 and (+)SKF10047 bind Sigma1 with affinities (K_i values) of 2 nM and 40 nM, respectively (Narayanan et al., 2011). However, only IPAG and haloperidol elicit UPR and autophagy. Although pharmacological properties of these prototypic compounds are described in considerable detail (Hayashi and Su, 2008; Spruce et al., 2004; Su et al., 2010), the molecular mechanisms of Sigma1 ligand actions are largely unknown and intracellular signaling pathways activated in response to ligand treatment are not well defined. Furthermore, although PRE-084 and (+)SKF10047 do not alter cell proliferation or survival, some putative agonists such as 4-IBP have been reported to have cytostatic properties as well as sensitize cancer cells to proapoptotic and proautophagic drugs (Megalizzi et al., 2009; Megalizzi et al., 2007). Because the functional domains that mediate Sigma1 actions have not been clearly identified, it remains difficult to use biochemical approaches to determine how putative agonist and antagonist binding specifically modulate Sigma1 functions. Indeed, the agonist and antagonist designations of many Sigma1 compounds are based primarily on data from rodent behavior assays (Su et al., 2010). Thus, the difference between putative antagonist and putative agonist responses remains unresolved at the molecular and cellular level. It is noteworthy that Sigma1 does not have the properties of a traditional receptor, and therefore designation of Sigma1 selective compounds as classically defined receptor antagonist or agonist may be inaccurate. We propose that structure-activity relationship studies to identify chemotypes with Sigma1-mediated ER stress response inducing activities, regardless of antagonist or agonist designation, should be particularly informative in understanding the utility of Sigma1 ligands as cancer therapeutic agents.

Of the two proposed sigma receptor subtypes, the sigma1 receptor (Sigma1) has been cloned and widely characterized, and the sigma2 receptor subtype has remained a pharmacologically

defined entity until recently. Xu and colleagues have identified the PGRMC1 protein complex as the putative sigma2 receptor (Xu et al., 2011). A growing body of evidence demonstrates the anti-neoplastic activities of compounds with affinity for sigma2 receptor as well as Sigma1, and many ligands bind both Sigma1 and the sigma2 receptor with varying affinities for each subtype (Crawford and Bowen, 2002; Narayanan et al., 2011; Spruce et al., 2004; Su et al., 2010). However, here we find that knockdown of PGRMC1 with siRNA does not alter IPAG induction of BiP (marker of UPR) and has no effect or a modest effect on LC3II levels (marker of autophagosome formation), in further support of Sigma1 as the principal mediator of these responses in our model (Supplemental Figure 3). Therefore, Sigma1 and sigma2 receptor ligand mediated proliferation arrest and cell death of transformed cells may engage distinct cellular pathways.

Whether Sigma1 ligand induced ER stress is a direct or indirect effect is also unclear. Either the proteins associated with Sigma1 are directly altered by ligand binding, causing deleterious protein folding or other processing (directly implicating Sigma1 as a chaperone or as a molecular scaffold), or Sigma1 ligand binding may indirectly cause protein-folding defects leading to the subsequent activation of ER stress response pathways. For example, altered ER calcium levels can lead to protein mis-folding and subsequent UPR (Hoyer-Hansen and Jaattela, 2007; Ron and Walter, 2007; Schroder and Kaufman, 2005; Xu et al., 2005). Treatment with some Sigma1 ligands has been shown to modulate cytosolic calcium levels (Brent et al., 1996; Hayashi and Su, 2007). Recent evidence (Brimson et al., 2011) demonstrates that IPAG induced intracellular calcium release occurs at concentrations that clearly exceed the UPR and autophagy activating concentrations presented herein (Fig. 1, 3, 4). Therefore, it remains to be determined whether

Sigma1 ligand induced ER stress and UPR are caused by ER calcium release, or whether ER calcium release occurs as a result of Sigma1-ligand binding induced protein folding defects.

Regarding the rapid kinetics of Sigma antagonist actions upon “wash-out” of drugs, we propose at least two possibilities: (1) Sigma1 ligand induced stress requires continuous ligand-receptor binding to continuously inhibit basal chaperone-protein associations; or (2) continuous Sigma1 ligand binding maintains chaperone-protein associations that sustain ER stress response. No evidence of either has been reported, however, the rapid reversibility of Sigma1 ligand induced autophagy and the rapid disappearance of autophagosomes upon removal of drugs suggests that continuous treatment, and presumably constant intracellular IPAG binding, is necessary to sustain disruption of ER protein homeostasis. The availability of sufficient free compound within the cell to act on intracellular targets may also explain why concentrations of IPAG significantly higher than its binding affinity (K_d) are required for the cellular responses observed here and in the literature. This notion, applied to other compounds, is reviewed in detail elsewhere (Trainor, 2007).

Cytoprotective UPR and autophagy reach maximal levels in a dose and time-responsive manner (Fig. 1, 3, 4). Apoptotic cell death occurs when these levels are reached and sustained, presumably beyond the cellular capacity to suppress proteotoxic stress. Consistent with the notion that autophagy is a survival response to Sigma1 ligand induced ER stress, siRNA mediated knockdown of Beclin1 or ATG5 inhibits IPAG-induced autophagosome formation and facilitates apoptotic cell death (Fig. 2, 7, and Supplemental Figure 2). Beclin1 and ATG5 siRNA mediated knockdown both suppressed Sigma1 ligand induced GFP-positive puncta, demonstrating that components canonically associated with autophagosome formation are involved in Sigma1 mediated autophagic sequestration. However, whether Sigma1 ligand

induced autophagy corresponds with macroautophagy or a novel ER-associated sequestration and bulk degradation mechanism remains to be determined. The link between UPR and autophagy has been demonstrated using thapsigargin-induced ER stress (Ogata et al., 2006; Yorimitsu et al., 2006). However, we find that siRNA knockdown of Sigma1 does not inhibit thapsigargin (TG) induced UPR and autophagy (Supplemental Figure 4). This suggests that ER stress mediated autophagosome formation may vary according to the effector used to disrupt ER homeostasis.

Interestingly, the dose-response and time-action curves reveal that at lower drug concentrations, IPAG activates the UPR but do not induce autophagy (Fig. 3-4). Furthermore, at these doses it does not induce cell death. This suggests that below threshold stress levels, the UPR may be sufficient to preserve cell survival, and that lethal cytotoxicity occurs when Sigma1 ligand treatment exceeds these thresholds. As Sigma1 is enriched in the ER and its putative antagonists activate UPR and autophagy, our data suggest that Sigma1 functions as a regulatory component of ER protein homeostasis or proteostasis. Thus, these Sigma1 ligands are reminiscent of so-called proteostasis regulators that modulate ER protein folding capacity by coordinating the transcription and translation of chaperones that facilitate proper protein folding and transport in the ER (Mu et al., 2008). Together, these findings point to the potential utility of novel chemotherapeutic drug combinations including Sigma1 ligands in combination therapies designed to modulate protein synthesis, processing, and assembly, and degradation, without necessarily inducing cell death. These data suggest that Sigma1 ligand doses, treatment timing, and combinations can be controlled to increase the therapeutic utility of these small molecules beyond their use as cytotoxic agents. We believe that rationally designed Sigma1 ligand based

therapies will require a better understanding of the molecular mechanisms that govern Sigma1 regulation of cellular stress and homeostasis.

ACKNOWLEDGMENTS

We thank Dr. Francis Weiss-Garcia (MSKCC Monoclonal Antibody Core Facility) for assistance in generating the Sigma1 antibody, and we thank members of the Kim lab for technical assistance.

AUTHOR CONTRIBUTIONS

Participated in research design: Kim

Conducted experiments: Kim, Schrock, Stabler, Spino, Longen, Marino

Performed data analysis: Kim, Schrock

Wrote or contributed to the writing of the manuscript: Kim, Schrock, Pasternak

REFERENCES

- Aydar E, Onganer P, Perrett R, Djamgoz MB and Palmer CP (2006) The expression and functional characterization of sigma (σ) 1 receptors in breast cancer cell lines. *Cancer Lett* **242**(2):245-257.
- Aydar E, Palmer CP, Klyachko VA and Jackson MB (2002) The sigma receptor as a ligand-regulated auxiliary potassium channel subunit. *Neuron* **34**(3):399-410.
- Bernales S, McDonald KL and Walter P (2006) Autophagy counterbalances endoplasmic reticulum expansion during the unfolded protein response. *PLoS Biol* **4**(12):e423.
- Bernales S, Schuck S and Walter P (2007) ER-phagy: selective autophagy of the endoplasmic reticulum. *Autophagy* **3**(3):285-287.
- Berthois Y, Bourrie B, Galiegue S, Vidal H, Carayon P, Martin PM and Casellas P (2003) SR31747A is a sigma receptor ligand exhibiting antitumoural activity both in vitro and vivo. *Br J Cancer* **88**(3):438-446.
- Brent PJ, Pang G, Little G, Dosen PJ and Van Helden DF (1996) The sigma receptor ligand, reduced haloperidol, induces apoptosis and increases intracellular-free calcium levels $[Ca^{2+}]_i$ in colon and mammary adenocarcinoma cells. *Biochem Biophys Res Commun* **219**(1):219-226.
- Brimson JM, Brown CA and Safrany ST (2011) Antagonists show GTP-sensitive high-affinity binding to the sigma-1 receptor. *Br J Pharmacol* **164**(2b):772-780.
- Crawford KW and Bowen WD (2002) Sigma-2 receptor agonists activate a novel apoptotic pathway and potentiate antineoplastic drugs in breast tumor cell lines. *Cancer Res* **62**(1):313-322.
- Degenhardt K, Mathew R, Beaudoin B, Bray K, Anderson D, Chen G, Mukherjee C, Shi Y, Gelinas C, Fan Y, Nelson DA, Jin S and White E (2006) Autophagy promotes tumor cell survival and restricts necrosis, inflammation, and tumorigenesis. *Cancer Cell* **10**(1):51-64.
- Hanner M, Moebius FF, Flandorfer A, Knaus HG, Striessnig J, Kempner E and Glossmann H (1996) Purification, molecular cloning, and expression of the mammalian sigma1-binding site. *Proc Natl Acad Sci U S A* **93**(15):8072-8077.
- Hayashi T and Su TP (2007) Sigma-1 receptor chaperones at the ER-mitochondrion interface regulate Ca^{2+} signaling and cell survival. *Cell* **131**(3):596-610.
- Hayashi T and Su TP (2008) An update on the development of drugs for neuropsychiatric disorders: focusing on the sigma 1 receptor ligand. *Expert Opin Ther Targets* **12**(1):45-58.
- He C and Klionsky DJ (2009) Regulation mechanisms and signaling pathways of autophagy. *Annu Rev Genet* **43**:67-93.
- Hippert MM, O'Toole PS and Thorburn A (2006) Autophagy in cancer: good, bad, or both? *Cancer Res* **66**(19):9349-9351.
- Hosokawa N, Hara Y and Mizushima N (2006) Generation of cell lines with tetracycline-regulated autophagy and a role for autophagy in controlling cell size. *FEBS Lett* **580**(11):2623-2629.
- Hoyer-Hansen M and Jaattela M (2007) Connecting endoplasmic reticulum stress to autophagy by unfolded protein response and calcium. *Cell Death Differ* **14**(9):1576-1582.
- Jonikas MC, Collins SR, Denic V, Oh E, Quan EM, Schmid V, Weibezahn J, Schwappach B, Walter P, Weissman JS and Schuldiner M (2009) Comprehensive characterization of

- genes required for protein folding in the endoplasmic reticulum. *Science* **323**(5922):1693-1697.
- Kim FJ, Schrock JM, Spino CM, Marino JC and Pasternak GW (2012) Inhibition of tumor cell growth by Sigma1 ligand mediated translational repression. *Biochem Biophys Res Commun.*
- Kim I, Xu W and Reed JC (2008) Cell death and endoplasmic reticulum stress: disease relevance and therapeutic opportunities. *Nat Rev Drug Discov* **7**(12):1013-1030.
- Kimes AS, Wilson AA, Scheffel U, Campbell BG and London ED (1992) Radiosynthesis, cerebral distribution, and binding of [¹²⁵I]-1-(p-iodophenyl)-3-(1-adamantyl)guanidine, a ligand for sigma binding sites. *J Med Chem* **35**(25):4683-4689.
- Klionsky DJ, Abeliovich H, Agostinis P, Agrawal DK, Aliev G, Askew DS, Baba M, Baehrecke EH, Bahr BA, Ballabio A, Bamber BA, Bassham DC, Bergamini E, Bi X, Biard-Piechaczyk M, Blum JS, Bredesen DE, Brodsky JL, Brumell JH, Brunk UT, Bursch W, Camougrand N, Cebollero E, Cecconi F, Chen Y, Chin LS, Choi A, Chu CT, Chung J, Clarke PG, Clark RS, Clarke SG, Clave C, Cleveland JL, Codogno P, Colombo MI, Coto-Montes A, Cregg JM, Cuervo AM, Debnath J, Demarchi F, Dennis PB, Dennis PA, Deretic V, Devenish RJ, Di Sano F, Dice JF, Difiglia M, Dinesh-Kumar S, Distelhorst CW, Djavaheri-Mergny M, Dorsey FC, Droge W, Dron M, Dunn WA, Jr., Duszenko M, Eissa NT, Elazar Z, Esclatine A, Eskelinen EL, Fesus L, Finley KD, Fuentes JM, Fueyo J, Fujisaki K, Galliot B, Gao FB, Gewirtz DA, Gibson SB, Gohla A, Goldberg AL, Gonzalez R, Gonzalez-Estevez C, Gorski S, Gottlieb RA, Haussinger D, He YW, Heidenreich K, Hill JA, Hoyer-Hansen M, Hu X, Huang WP, Iwasaki A, Jaattela M, Jackson WT, Jiang X, Jin S, Johansen T, Jung JU, Kadowaki M, Kang C, Kelekar A, Kessel DH, Kiel JA, Kim HP, Kimchi A, Kinsella TJ, Kiselyov K, Kitamoto K, Knecht E, Komatsu M, Kominami E, Kondo S, Kovacs AL, Kroemer G, Kuan CY, Kumar R, Kundu M, Landry J, Laporte M, Le W, Lei HY, Lenardo MJ, Levine B, Lieberman A, Lim KL, Lin FC, Liou W, Liu LF, Lopez-Berestein G, Lopez-Otin C, Lu B, Macleod KF, Malorni W, Martinet W, Matsuoka K, Mautner J, Meijer AJ, Melendez A, Michels P, Miotto G, Mistiaen WP, Mizushima N, Mograbi B, Monastyrska I, Moore MN, Moreira PI, Moriyasu Y, Motyl T, Munz C, Murphy LO, Naqvi NI, Neufeld TP, Nishino I, Nixon RA, Noda T, Nurnberg B, Ogawa M, Oleinick NL, Olsen LJ, Ozpolat B, Paglin S, Palmer GE, Papassideri I, Parkes M, Perlmutter DH, Perry G, Piacentini M, Pinkas-Kramarski R, Prescott M, Proikas-Cezanne T, Raben N, Rami A, Reggiori F, Rohrer B, Rubinsztein DC, Ryan KM, Sadoshima J, Sakagami H, Sakai Y, Sandri M, Sasakawa C, Sass M, Schneider C, Seglen PO, Seleverstov O, Settleman J, Shacka JJ, Shapiro IM, Sibirny A, Silva-Zacarin EC, Simon HU, Simone C, Simonsen A, Smith MA, Spanel-Borowski K, Srinivas V, Steeves M, Stenmark H, Stromhaug PE, Subauste CS, Sugimoto S, Sulzer D, Suzuki T, Swanson MS, Tabas I, Takeshita F, Talbot NJ, Talloczy Z, Tanaka K, Tanaka K, Tanida I, Taylor GS, Taylor JP, Terman A, Tettamanti G, Thompson CB, Thumm M, Tolkovsky AM, Tooze SA, Truant R, Tumanovska LV, Uchiyama Y, Ueno T, Uzcategui NL, van der Klei I, Vaquero EC, Vellai T, Vogel MW, Wang HG, Webster P, Wiley JW, Xi Z, Xiao G, Yahalom J, Yang JM, Yap G, Yin XM, Yoshimori T, Yu L, Yue Z, Yuzaki M, Zabirnyk O, Zheng X, Zhu X and Deter RL (2008) Guidelines for the use and interpretation of assays for monitoring autophagy in higher eukaryotes. *Autophagy* **4**(2):151-175.

- Kuma A, Matsui M and Mizushima N (2007) LC3, an autophagosome marker, can be incorporated into protein aggregates independent of autophagy: caution in the interpretation of LC3 localization. *Autophagy* **3**(4):323-328.
- Levine B and Klionsky DJ (2004) Development by self-digestion: molecular mechanisms and biological functions of autophagy. *Dev Cell* **6**(4):463-477.
- Levine B and Kroemer G (2008) Autophagy in the pathogenesis of disease. *Cell* **132**(1):27-42.
- Marciniak SJ and Ron D (2006) Endoplasmic reticulum stress signaling in disease. *Physiol Rev* **86**(4):1133-1149.
- Martin WR, Eades CG, Thompson JA, Huppler RE and Gilbert PE (1976) The effects of morphine- and nalorphine- like drugs in the nondependent and morphine-dependent chronic spinal dog. *J Pharmacol Exp Ther* **197**(3):517-532.
- Mathew R, Karp CM, Beaudoin B, Vuong N, Chen G, Chen HY, Bray K, Reddy A, Bhanot G, Gelinas C, Dipaola RS, Karantza-Wadsworth V and White E (2009) Autophagy suppresses tumorigenesis through elimination of p62. *Cell* **137**(6):1062-1075.
- Megalizzi V, Decaestecker C, Debeir O, Spiegl-Kreinecker S, Berger W, Lefranc F, Kast RE and Kiss R (2009) Screening of anti-glioma effects induced by sigma-1 receptor ligands: potential new use for old anti-psychiatric medicines. *Eur J Cancer* **45**(16):2893-2905.
- Megalizzi V, Mathieu V, Mijatovic T, Gailly P, Debeir O, De Neve N, Van Damme M, Bontempi G, Haibe-Kains B, Decaestecker C, Kondo Y, Kiss R and Lefranc F (2007) 4-IBP, a sigma1 receptor agonist, decreases the migration of human cancer cells, including glioblastoma cells, in vitro and sensitizes them in vitro and in vivo to cytotoxic insults of proapoptotic and proautophagic drugs. *Neoplasia* **9**(5):358-369.
- Mizushima N, Levine B, Cuervo AM and Klionsky DJ (2008) Autophagy fights disease through cellular self-digestion. *Nature* **451**(7182):1069-1075.
- Mizushima N and Yoshimori T (2007) How to interpret LC3 immunoblotting. *Autophagy* **3**(6):542-545.
- Mu TW, Ong DS, Wang YJ, Balch WE, Yates JR, 3rd, Segatori L and Kelly JW (2008) Chemical and biological approaches synergize to ameliorate protein-folding diseases. *Cell* **134**(5):769-781.
- Narayanan S, Bhat R, Mesangeau C, Poupaert JH and McCurdy CR (2011) Early development of sigma-receptor ligands. *Future Med Chem* **3**(1):79-94.
- Ni M and Lee AS (2007) ER chaperones in mammalian development and human diseases. *FEBS Lett* **581**(19):3641-3651.
- Ogata M, Hino S, Saito A, Morikawa K, Kondo S, Kanemoto S, Murakami T, Taniguchi M, Tanii I, Yoshinaga K, Shiosaka S, Hammarback JA, Urano F and Imaizumi K (2006) Autophagy is activated for cell survival after endoplasmic reticulum stress. *Mol Cell Biol* **26**(24):9220-9231.
- Piergentili A, Amantini C, Del Bello F, Giannella M, Mattioli L, Palmery M, Perfumi M, Pignini M, Santoni G, Tucci P, Zotti M and Quaglia W Novel highly potent and selective sigma 1 receptor antagonists related to spipethiane. *J Med Chem* **53**(3):1261-1269.
- Ron D and Walter P (2007) Signal integration in the endoplasmic reticulum unfolded protein response. *Nat Rev Mol Cell Biol* **8**(7):519-529.
- Rubinsztein DC, Gestwicki JE, Murphy LO and Klionsky DJ (2007) Potential therapeutic applications of autophagy. *Nat Rev Drug Discov* **6**(4):304-312.
- Ryan-Moro J, Chien CC, Standifer KM and Pasternak GW (1996) Sigma binding in a human neuroblastoma cell line. *Neurochem Res* **21**(11):1309-1314.

- Schroder M and Kaufman RJ (2005) The mammalian unfolded protein response. *Annu Rev Biochem* **74**:739-789.
- Scott RC, Juhasz G and Neufeld TP (2007) Direct induction of autophagy by Atg1 inhibits cell growth and induces apoptotic cell death. *Curr Biol* **17**(1):1-11.
- Solimini NL, Luo J and Elledge SJ (2007) Non-oncogene addiction and the stress phenotype of cancer cells. *Cell* **130**(6):986-988.
- Spruce BA, Campbell LA, McTavish N, Cooper MA, Appleyard MV, O'Neill M, Howie J, Samson J, Watt S, Murray K, McLean D, Leslie NR, Safrany ST, Ferguson MJ, Peters JA, Prescott AR, Box G, Hayes A, Nutley B, Raynaud F, Downes CP, Lambert JJ, Thompson AM and Eccles S (2004) Small molecule antagonists of the sigma-1 receptor cause selective release of the death program in tumor and self-reliant cells and inhibit tumor growth in vitro and in vivo. *Cancer Res* **64**(14):4875-4886.
- Su TP, Hayashi T, Maurice T, Buch S and Ruoho AE (2010) The sigma-1 receptor chaperone as an inter-organelle signaling modulator. *Trends Pharmacol Sci* **31**(12):557-566.
- Szegezdi E, Logue SE, Gorman AM and Samali A (2006) Mediators of endoplasmic reticulum stress-induced apoptosis. *EMBO Rep* **7**(9):880-885.
- Trainor GL (2007) The importance of plasma protein binding in drug discovery. *Expert Opin Drug Discov* **2**(1):51-64.
- Vilner BJ, de Costa BR and Bowen WD (1995a) Cytotoxic effects of sigma ligands: sigma receptor-mediated alterations in cellular morphology and viability. *J Neurosci* **15**(1 Pt 1):117-134.
- Vilner BJ, John CS and Bowen WD (1995b) Sigma-1 and sigma-2 receptors are expressed in a wide variety of human and rodent tumor cell lines. *Cancer Res* **55**(2):408-413.
- Webber JL and Tooze SA (2010) Coordinated regulation of autophagy by p38alpha MAPK through mAtg9 and p38IP. *EMBO J* **29**(1):27-40.
- Wolozin BL, Nishimura S and Pasternak GW (1982) The binding of kappa- and sigma-opiates in rat brain. *J Neurosci* **2**(6):708-713.
- Xu C, Bailly-Maitre B and Reed JC (2005) Endoplasmic reticulum stress: cell life and death decisions. *J Clin Invest* **115**(10):2656-2664.
- Xu J, Zeng C, Chu W, Pan F, Rothfuss JM, Zhang F, Tu Z, Zhou D, Zeng D, Vangveravong S, Johnston F, Spitzer D, Chang KC, Hotchkiss RS, Hawkins WG, Wheeler KT and Mach RH (2011) Identification of the PGRMC1 protein complex as the putative sigma-2 receptor binding site. *Nat Commun* **2**:380.
- Yorimitsu T, Nair U, Yang Z and Klionsky DJ (2006) Endoplasmic reticulum stress triggers autophagy. *J Biol Chem* **281**(40):30299-30304.

FOOTNOTES

This work was supported in part by a Kimmel Cancer Center – Thomas Jefferson University – Drexel University Consortium Pilot Study Award; grants from the National Institutes of Health National Institute on Drug Abuse [Grants DA06241, DA02615, DA07274]; an award from the Mr. William H. Goodwin and Mrs. Alice Goodwin and the Commonwealth Foundation for Cancer Research and The Experimental Therapeutics Center of Memorial Sloan-Kettering Cancer Center; and a grant from the Translational and Integrative Medicine Fund of Memorial Sloan-Kettering Cancer Center.

LEGENDS FOR FIGURES

Figure 1. Sigma1 ligand treatment associated autophagosome formation and autophagic flux. **A.)** Translocation of GFP-tagged LC3 (GFP-LC3) into autophagosomes in Sigma1 ligand treated MDA-MB-468(GFP-LC3) cells. Cells were treated for 24 hours with DMSO (vehicle), 10 μ M IPAG or haloperidol (putative antagonists), or with 50 μ M PRE-084 or (+)SKF10047 (putative agonists). (+)SKF10047 is abbreviated as (+)SKF. Basal indicates no treatment. **B.)** GFP-LC3 puncta were quantified in MDA-MB-468(GFP-LC3) cells treated as in A.). Histograms represent data from at least four determinations, and are presented as the mean number \pm S.E.M of puncta per cell at the indicated doses of drug. Data are representative of at least 10 fields and 300 cells for each drug at each concentration. ***p < 0.001 for both IPAG and haloperidol compared to basal, DMSO, PRE-084, and (+)SKF10047 treatment conditions. **C.)** Cleavage of GFP-LC3 was used to evaluate autophagic flux. MDA-MB-468(GFP-LC3) cells were treated for 24 hours with the indicated Sigma1 ligands, and detergent soluble whole-cell lysates were immunoblotted with an anti-GFP antibody to demonstrate cleavage and release of cleaved GFP. **D.)** Immunoblot demonstrating inhibition of GFP-LC3 cleavage in presence of 10nM Bafilomycin A1 (Baf A1). MDA-MB-468(GFP-LC3) treated for 12 hours with DMSO, IPAG (10 μ M), Baf A1 (10 nM), with DMSO or IPAG (10 μ M) combined with Baf A1 (10nM) for the final 2 hours of the 12 hour treatment. **E.)** Representative fluorescent micrographs of GFP-LC3 puncta in MDA-MB-468(GFP-LC3) treated as described in D.), above. **F.)** Quantification of GFP-LC3 positive puncta in E.). **G.)** Immunoblot of LC3II levels in MDA-MB-468 breast adenocarcinoma cells treated for 24 hours with 10 μ M Sigma1 putative antagonists (IPAG, haloperidol) or 50 μ M putative agonists (PRE-084, (+)SKF10047). **H.)** LC3II immunoblot of cell lysates from the following cell lines treated for 24 hours with IPAG

(10 μ M) or PRE-084 (50 μ M): breast adenocarcinoma (MCF-7, T47D), prostate adenocarcinoma (PC3), hepatocellular carcinoma (HepG2), and pancreatic adenocarcinoma (Panc1).

Figure 2. Inhibition of Sigma1 ligand treatment associated autophagosome formation by siRNA knockdown of Beclin1 or ATG5. *A-C.)* Beclin1 or control siRNA was transfected 72 hours prior to treatment with IPAG. Cells were treated for 24 hours with 10 μ M IPAG. *A.)* Immunoblot to confirm siRNA knockdown of Beclin1. *B.)* Representative images of MDA-MB-468(GFP-LC3) cells treated as described above. *C.)* Quantification of images as mean number of GFP-LC3 puncta per cell. Data are representative of at least 10 fields and 200 cells for each treatment condition. *D-F.)* ATG5 or control siRNA was transfected twice, 90 hours prior to treatment with IPAG. Cells were treated for 24 hours with 10 μ M IPAG. *D.)* Immunoblot to confirm siRNA knockdown of ATG5. *E.)* Representative images of MDA-MB-468(GFP-LC3) cells treated as described above. *F.)* Quantification of images as mean number of GFP-LC3 puncta per cell.

Figure 3. Dose-responsive induction of UPR by Sigma1 ligand. MDA-MB-468 cells were treated for 24 hours with increasing doses of IPAG (1 to 20 μ M). *A.)* Induction of BiP protein levels. *B.)* Phosphorylation of p38MAPK (Thr180/Tyr182). *C.)* Induction of IRE1 α protein levels and phosphorylation of JNK (Thr183/Tyr185). *D.)* Phosphorylation of PERK (phospho-PERK, P-PERK), induction of ATF4 protein levels, and phosphorylation of eIF2 α (Ser51). *E.)* Induction of LC3II protein levels. *F.)* Immunoblot revealing Sigma1 protein levels. *G.)* Quantification of autophagosomes and UPR marker induction following 24-hour treatment with 1 μ M IPAG. Data generated from at least three independent determinations, and are presented as

mean fold induction over DMSO treated control. Error bars represent the standard error of the mean. * $p < 0.05$; *** $p < 0.001$.

Figure 4. Time-course of Sigma1 ligand induced UPR and autophagy. Time-course of Sigma1 antagonist-induced ER stress was evaluated by immunoblot analysis of UPR markers. Cells were treated for indicated times with 10 μ M IPAG. **A.)** Induction of IRE1 α protein levels and phosphorylation of JNK (Thr183/Tyr185). **B.)** Phosphorylation of PERK (phospho-PERK, P-PERK), induction of ATF4 protein levels, and phosphorylation of eIF2 α (Ser51). **C.)** Phosphorylation of p38MAPK (Thr180/Tyr182). **D.)** Induction of BiP protein levels. **E.)** Time-action histogram of autophagosome formation in MDA-MB-468(GFP-LC3). Data are representative of at least 10 fields and 300 cells for each drug concentration. $p < 0.001$ for 24 hour IPAG treatment compared to 0 hour (basal), 1 hour, and 6 hour; $p < 0.05$ for 24 hour compared to 12 hour IPAG treatment. **F.)** Immunoblot revealing BCL2 protein levels. **G.)** Treatment of the following cell lines for 24 hours with IPAG (10 μ M) or PRE-084 (50 μ M) and immunoblot of detergent soluble whole-cell lysates with BiP antibody: breast adenocarcinoma (MCF-7, T47D), prostate adenocarcinoma (PC3), hepatocellular carcinoma (HepG2), and pancreatic adenocarcinoma (Panc1).

Figure 5. Sigma1 ligand mediated UPR and autophagy are Sigma1 dependent. MDA-MB-468 cells were treated for 24 hours with 10 μ M IPAG, 90 hours following two transfections with either control or Sigma1 siRNA. **A.)** [¹²⁵I] IPAG radioligand binding saturation curves in control siRNA transfected (solid line, closed squares) and Sigma1 knockdown (dashed line, open circles) cell membranes. Data are presented as mean \pm S.D. and are representative of three

determinations. Immunoblot confirming siRNA-mediated knockdown of Sigma1 is shown above the graph. **B.**) Immunoblot confirming siRNA-mediated knockdown of Sigma1 post-transfection and treatment in MDA-MB-468 cells and detection of Sigma1 and UPR markers BiP, IRE1 α , and ATF4. Immunoblot is representative of three determinations. **C-D.**) GFP-LC3 puncta formation in MDA-MB-468(GFP-LC3) cells treated for 24 hours with 10 μ M IPAG following siRNA mediated knockdown of Sigma1. Immunoblot of Sigma1 knockdown and representative fluorescent micrograph images are shown in **C.**) and GFP-LC3 puncta quantified in **D.**)

Figure 6. Inhibition of Sigma1 ligand mediated UPR inhibits autophagy. **A-B.**) Immunoblot of IRE1 α siRNA knockdown in **A.**) and ATF4 siRNA knockdown in **B.**). 72 h post-transfection., MDA-MB-468(GFP-LC3) cells were treated for 24 hours with a combination of IPAG (10 μ M). Knockdown of IRE1 α or ATF4 abrogates IPAG mediated induction of GFP-LC3 cleavage. **C.-D.**) siRNA mediated knockdown of IRE1 α and ATF4 abrogate GFP-LC3 puncta formation. Representative images in **C.**) and quantified in **D.**)

Figure 7. Inhibition of UPR or autophagy accelerates Sigma1 ligand induced apoptosis. **A.**) Time-course of IPAG-induced cell death (trypan blue exclusion). MDA-MB-468 cells were treated for 24 and 48 hours with 10 μ M IPAG, and compared to cells treated with 10 μ M PRE-084 or DMSO (control). Data are from at least 4 determinations (*** $p < 0.001$). **B.**) Immunoblot demonstrating Caspase 3 (Asp 175) cleavage (cCaspase) following 48 hours of IPAG treatment. **C.**) IPAG induced cell death in IRE1 α knockdown cells, 72 hours following transfection of IRE1 α siRNA. Data are from at least 4 determinations. **D.**) Immunoblot confirming siRNA mediated IRE1 α knockdown and demonstrating IPAG induced apoptosis by cleavage of caspase

3 (cCaspase) and PARP (cPARP). *E.*) IPAG-induced cell death measured in Beclin knockdown cells. Cells were treated for 16 hours with 10 μ M IPAG, 72 hours following transfection of Beclin siRNA. Cell death was quantified as in *A.*) *F.*) Apoptotic cell death was confirmed by immunoblot detection of cleaved caspase 3 (ccaspase) and cleaved PARP (cPARP) as in *B.*)

Figure 8. Reversibility of Sigma1 ligand induced UPR and autophagosome formation.

MDA-MB-468(GFP-LC3) cells were treated for 24 hours with 10 μ M IPAG. Subsequently, the treated cells were washed 3 times with complete medium (wash-out) and further cultured in drug-free complete medium for the indicated number of hours (recovery). *A.*) Representative fluorescent micrograph of MDA-MB-468(GFP-LC3) during treatment, wash-out, and recovery. *B.*) Quantification of GFP-LC3 puncta per cell. Data were quantified from four determinations, and are presented as mean \pm S.E.M. *C.*) Immunoblot of GFP-LC3 cleavage, demonstrating autophagic flux. *D.*) Immunoblot of UPR markers during treatment, wash-out, and recovery period. *E.*) Absence of detectable cell death during treatment and post-wash-out period measured by trypan blue exclusion assay.

Figure 1

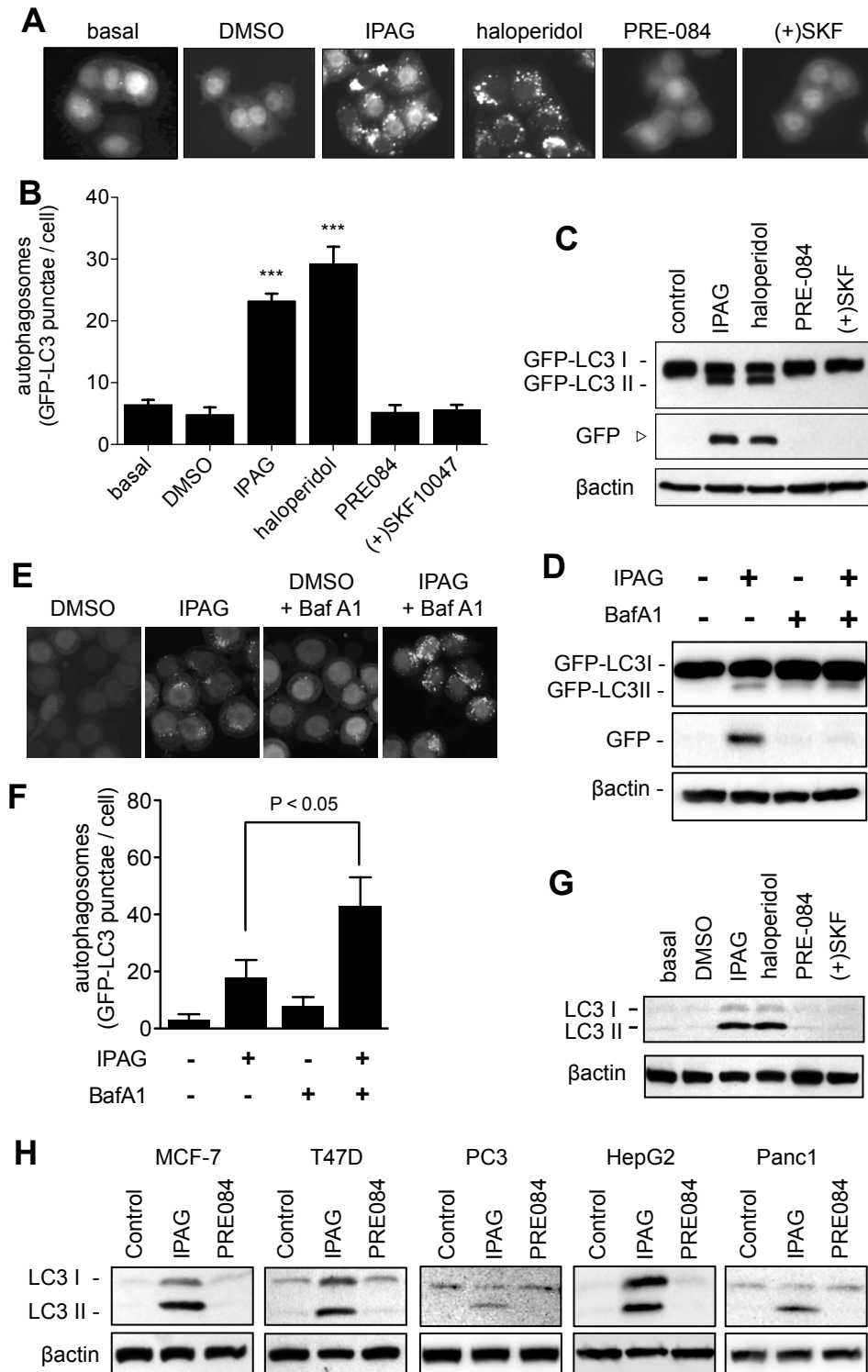


Figure 2

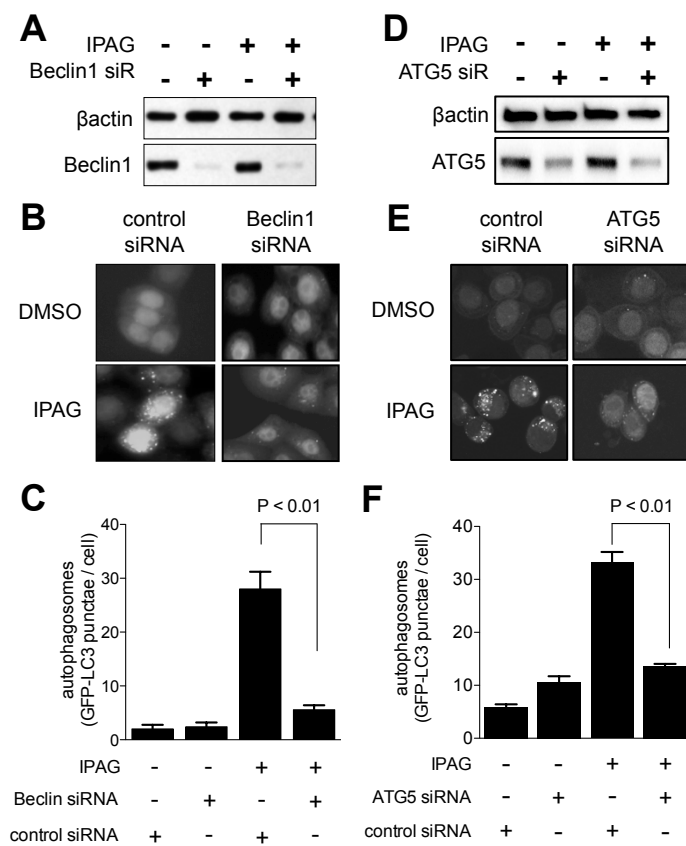


Figure 3

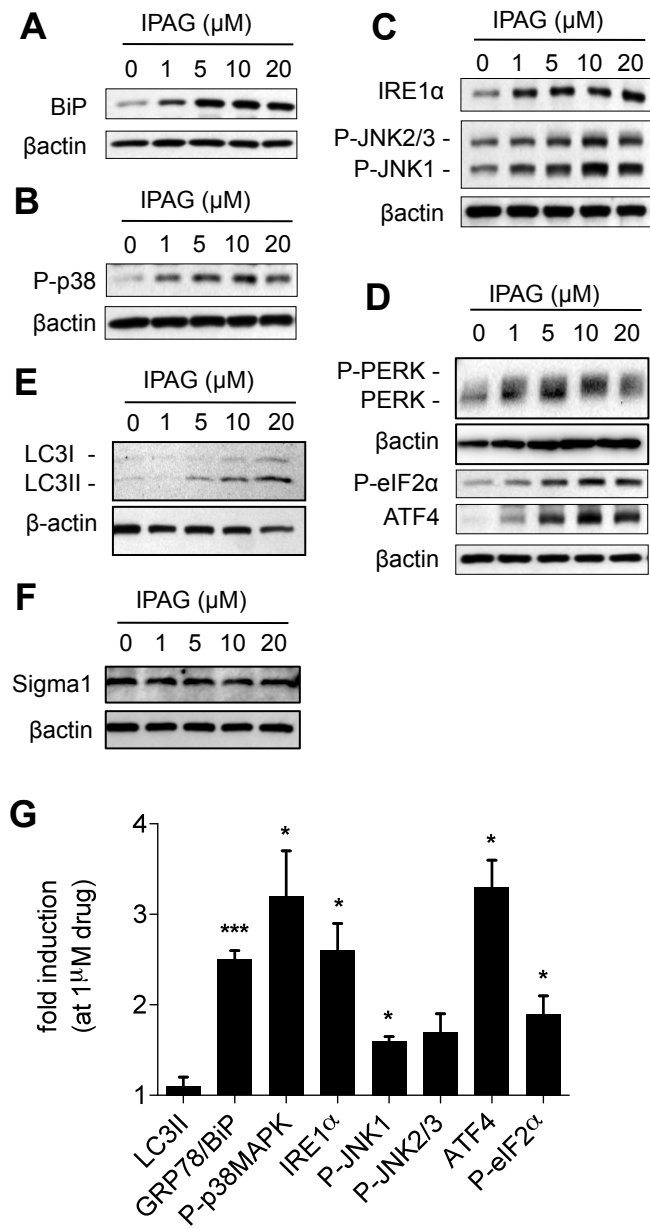


Figure 4

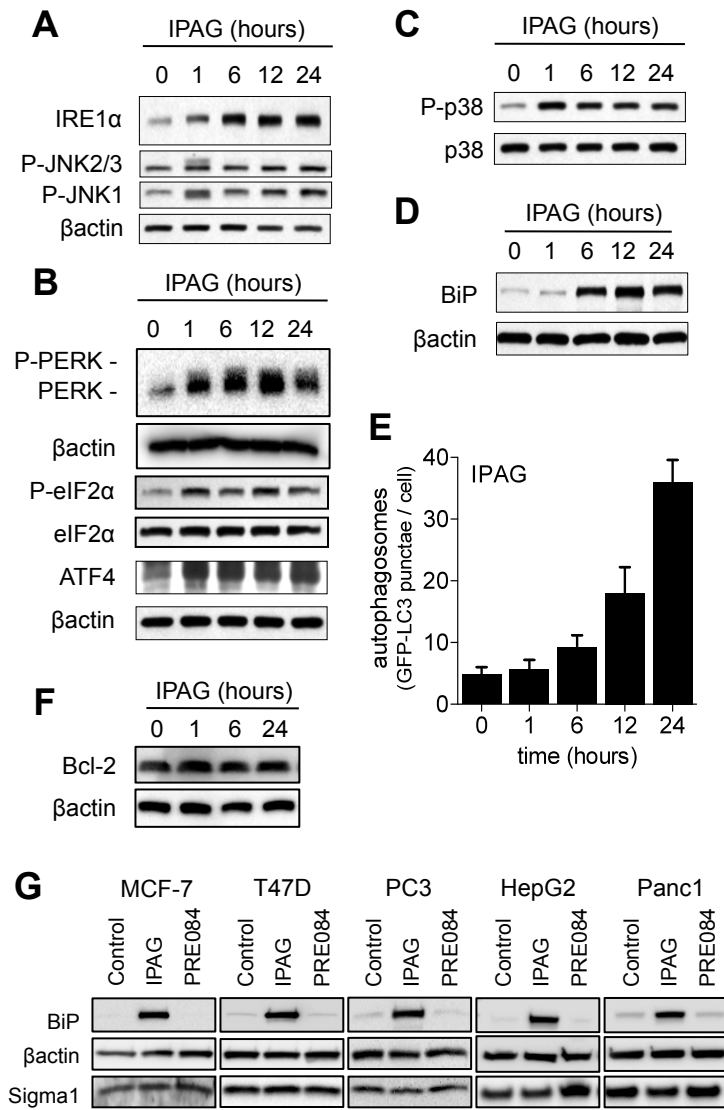


Figure 5

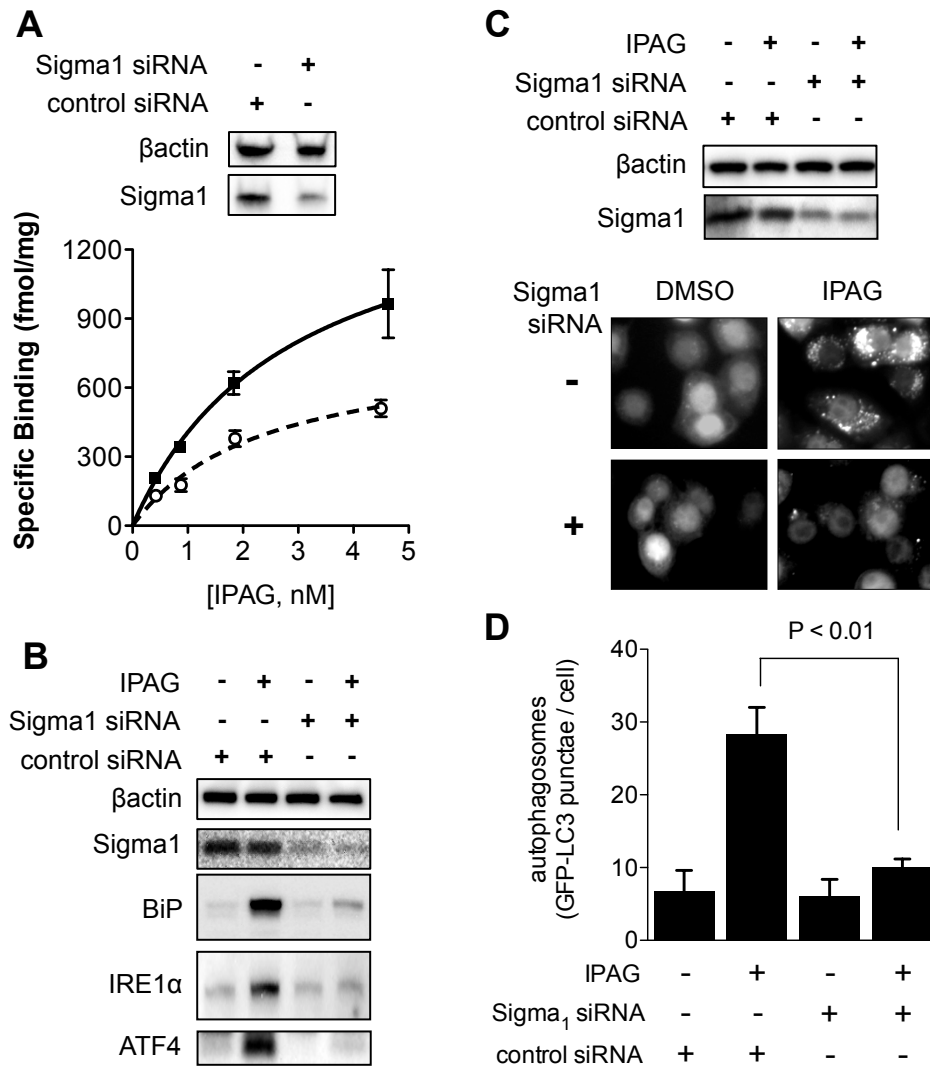


Figure 6

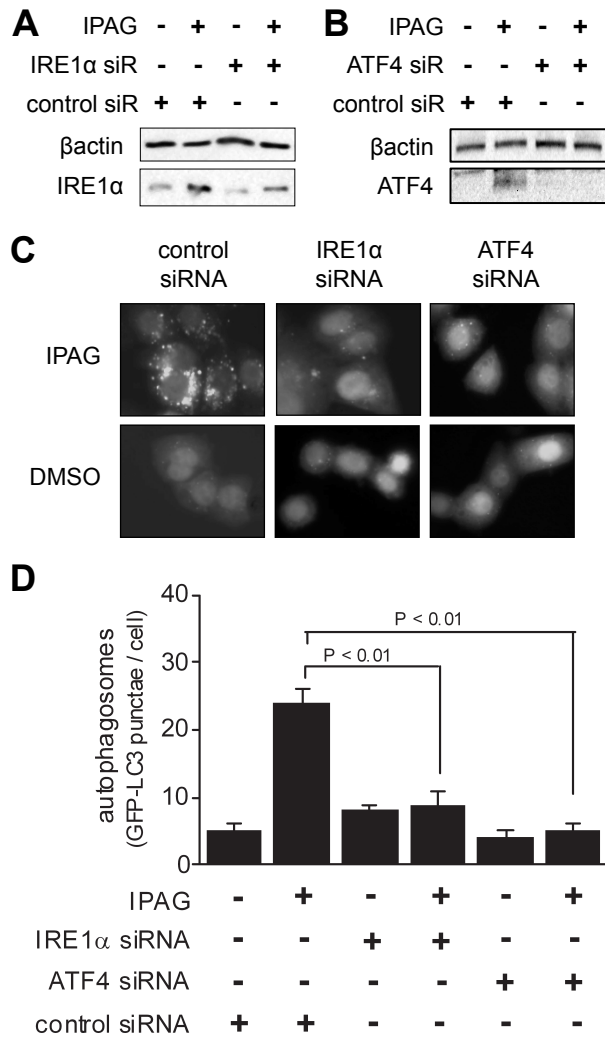


Figure 7

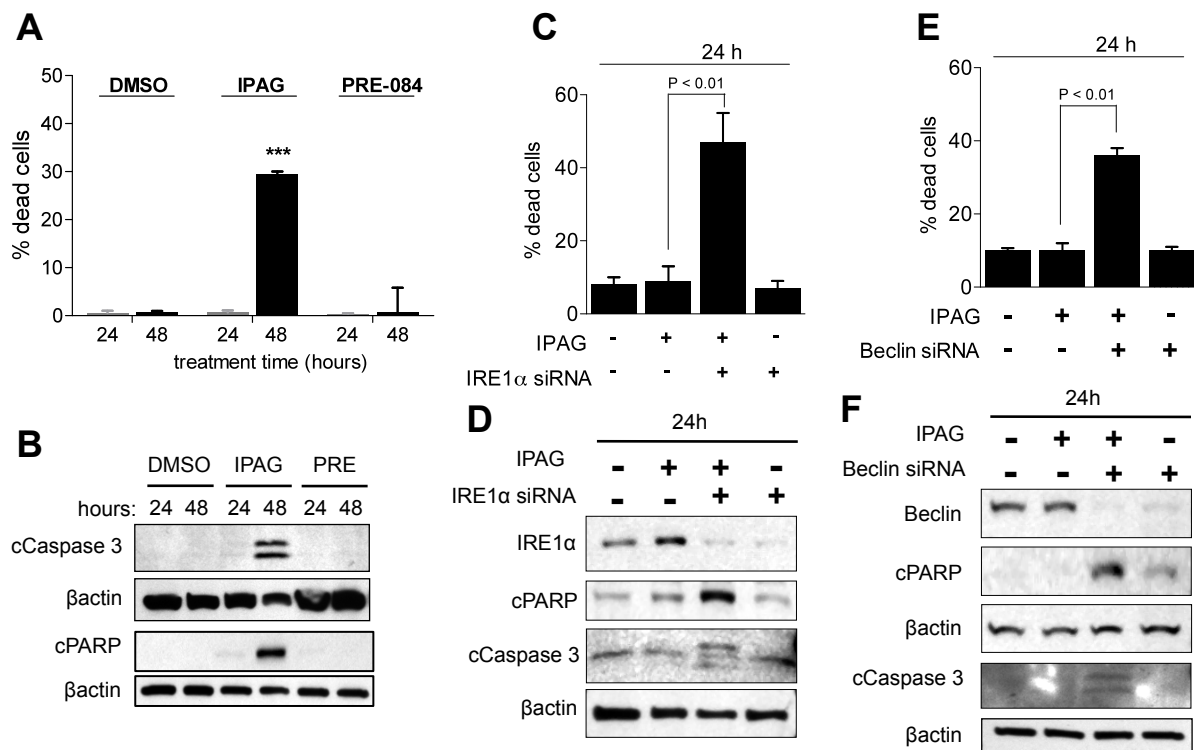


Figure 8

